

## Dioxygen Activation by Mononuclear Nonheme Iron(II) Complexes Generates Iron–Oxygen Intermediates in the Presence of an NADH Analogue and Proton

Seungwoo Hong,<sup>†,‡</sup> Yong-Min Lee,<sup>†</sup> Woonsup Shin,<sup>\*,‡</sup> Shunichi Fukuzumi,<sup>\*,§</sup> and Wonwoo Nam<sup>\*,†</sup>

Department of Chemistry and Nano Science, Department of Bioinspired Science, Ewha Womans University, Seoul 120-750, Korea, Department of Chemistry and Interdisciplinary Program of Integrated Biotechnology, Sogang University, Seoul 121-742, Korea, and Department of Material and Life Science, Graduate School of Engineering, Osaka University, SORST, Osaka 565-0871, Japan

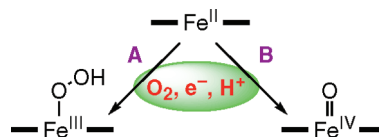
Received July 10, 2009; E-mail: shinws@sogang.ac.kr; fukuzumi@chem.eng.osaka-u.ac.jp; wwnam@ewha.ac.kr

One primary goal in biomimetic research is to understand mechanisms of dioxygen activation, structures of reactive intermediates, and reactivities of these intermediates in oxidation reactions by metalloenzymes such as heme and nonheme iron oxygenases.<sup>1</sup> Extensive mechanistic studies have been carried out on synthetic iron–oxygen adducts such as iron(III)-hydroperoxo and iron(IV)-oxo complexes, mostly formed using artificial oxidants such as iodosylarenes, peroxy acids, and H<sub>2</sub>O<sub>2</sub>.<sup>1</sup> However, enzymes instead use dioxygen and electrons plus protons or cofactors (e.g., a tetrahydropterin or an  $\alpha$ -keto acid) in generating iron–oxygen intermediates.<sup>2</sup> Therefore, the use of O<sub>2</sub> as the primary oxidant and oxygen source in studies on synthetic iron complexes is of fundamental importance. However, there are many intrinsic problems in this approach, and only a few examples exist.<sup>3–6</sup>

Nam and co-workers and Barse, Que and co-workers have independently reported the generation of nonheme iron(IV)-oxo complexes by activating O<sub>2</sub>.<sup>5,6</sup> The former group demonstrated the generation of [(TMC)Fe<sup>IV</sup>(O)]<sup>2+</sup> in the reaction of [Fe<sup>II</sup>(TMC)]<sup>2+</sup> and O<sub>2</sub> in solvent mixtures of CH<sub>3</sub>CN/alcohols or CH<sub>3</sub>CN/ethers,<sup>5,7</sup> whereas the latter group observed the formation of an iron(IV)-oxo complex in the reaction of [Fe<sup>II</sup>(TMC-py)]<sup>2+</sup> and O<sub>2</sub> in the presence of an electron (BPh<sub>4</sub><sup>−</sup>) and proton source (HClO<sub>4</sub>).<sup>6,7</sup> In those reactions, however, the formation of iron(III)-hydroperoxo species, which are precursors to the iron(IV)-oxo intermediates, was not observed. In the present work, we report the generation of nonheme iron(III)-hydroperoxo and iron(IV)-oxo intermediates by activating O<sub>2</sub> in the presence of a biologically important electron donor, a dihydronicotinamide adenine dinucleotide (NADH) analogue, and an acid; the formation of iron(III)-hydroperoxo and iron(IV)-oxo complexes was found to depend on the supporting ligands (Scheme 1, pathway A with N4Py and Bn-TPEN and pathway B with TMC; see ligand structures in the Supporting Information (SI), Figure S1).<sup>7</sup>

Low-spin iron(II) complexes bearing N4Py and Bn-TPEN ligands, [Fe<sup>II</sup>(N4Py)]<sup>2+</sup> and [Fe<sup>II</sup>(Bn-TPEN)]<sup>2+</sup>, are air-stable in CH<sub>3</sub>CN.<sup>8,9</sup> When we added 1-benzyl-1,4-dihydronicotinamide (BNAH; see structure in SI, Figure S1)<sup>10</sup> and HClO<sub>4</sub> to a CH<sub>3</sub>CN solution of [Fe<sup>II</sup>(N4Py)]<sup>2+</sup>, no reaction took place. Interestingly, when we dissolved [Fe<sup>II</sup>(N4Py)]<sup>2+</sup> in CH<sub>3</sub>OH and added BNAH and HClO<sub>4</sub> to the solution in the presence of O<sub>2</sub>, the color of the solution changed from yellow to purple within 3 min at 0 °C. By recording UV–vis and EPR spectra of the intermediate, we have confirmed the formation of [(N4Py)Fe<sup>III</sup>–OOH]<sup>2+</sup> (**1**) (Figure 1; also see SI, Figure S2 for spectral data of **1** prepared in the reaction of [Fe<sup>II</sup>(N4Py)]<sup>2+</sup> and H<sub>2</sub>O<sub>2</sub> in CH<sub>3</sub>OH).<sup>8</sup> The yield of **1** was determined to be ~90% by comparing the intensity of the absorption

### Scheme 1



band at 548 nm (Figure 1) with the known  $\epsilon$  value of **1**.<sup>8</sup> In addition, the yield of **1** was found to be maximal when 5 equiv of BNAH and 1.4 equiv of HClO<sub>4</sub> were added to the reaction solution (SI, Figure S3). Under these conditions and in an O<sub>2</sub>-saturated solution, the rate constant for this reaction,  $k_{\text{obs}}$ , was determined to be  $8.3 \times 10^{-3} \text{ s}^{-1}$ .<sup>11</sup> Similarly, the formation of [(Bn-TPEN)Fe<sup>III</sup>–OOH]<sup>2+</sup> (**2**) was not observed when [Fe<sup>II</sup>(Bn-TPEN)]<sup>2+</sup> reacted with O<sub>2</sub> in the presence of BNAH and HClO<sub>4</sub> in CH<sub>3</sub>CN. However, a change of solvent from CH<sub>3</sub>CN to CH<sub>3</sub>OH led to the formation of **2** (SI, Figure S4 for UV–vis and EPR spectra; also see Figure S5 for spectral data of **2** prepared in the reaction of [Fe<sup>II</sup>(Bn-TPEN)]<sup>2+</sup> and H<sub>2</sub>O<sub>2</sub> in CH<sub>3</sub>OH).<sup>9</sup> In these reactions, both BNAH and HClO<sub>4</sub> were required to generate the iron(III)-hydroperoxo complexes.

The activation of O<sub>2</sub> by [Fe<sup>II</sup>(TMC)]<sup>2+</sup> was also investigated in the presence of BNAH and HClO<sub>4</sub> in CH<sub>3</sub>CN. While [Fe<sup>II</sup>(TMC)]<sup>2+</sup> was air-stable in CH<sub>3</sub>CN,<sup>5</sup> it converted to [(TMC)Fe<sup>IV</sup>(O)]<sup>2+</sup> (**3**)<sup>12</sup> in >90% yield with a  $k_{\text{obs}}$  value of  $6.4 \times 10^{-3} \text{ s}^{-1}$  upon addition of 1 equiv each of BNAH and HClO<sub>4</sub> in CH<sub>3</sub>CN at room temperature (Figure 2).<sup>11</sup> In this reaction, the generation of [(TMC)Fe<sup>III</sup>–OOH]<sup>2+</sup> was not detected, probably due to this intermediate's instability. Indeed, it was shown previously that the reaction of [Fe<sup>II</sup>(TMC)]<sup>2+</sup> and H<sub>2</sub>O<sub>2</sub> afforded **3** rather than [(TMC)Fe<sup>III</sup>–OOH]<sup>2+</sup> in CH<sub>3</sub>CN.<sup>12</sup>

As shown above, solvent (i.e., alcohol) plays a key role in generating the iron(III)-hydroperoxo complexes in the reactions of

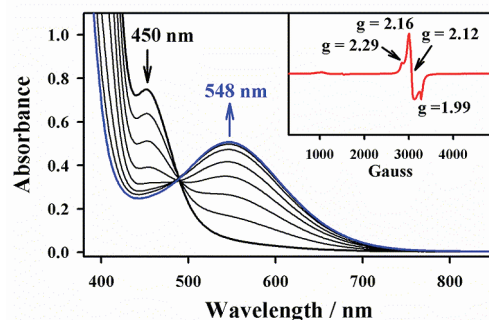


**Figure 1.** UV-vis spectral changes showing the formation of **1** (blue line) in the reaction of [Fe<sup>II</sup>(N4Py)](ClO<sub>4</sub>)<sub>2</sub> (0.5 mM) and O<sub>2</sub> in the presence of BNAH (0.7 mM) and HClO<sub>4</sub> (2.5 mM) in CH<sub>3</sub>OH at 0 °C. Inset shows X-band EPR spectrum of **1** (1.0 mM) at 4 K.

<sup>†</sup> Ewha Womans University.

<sup>‡</sup> Sogang University.

<sup>§</sup> Osaka University.

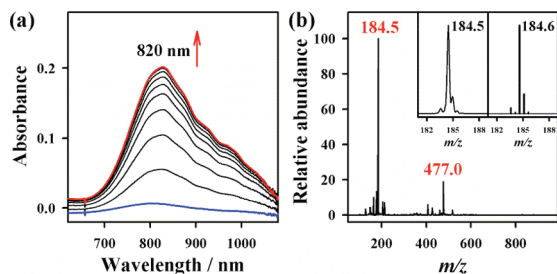
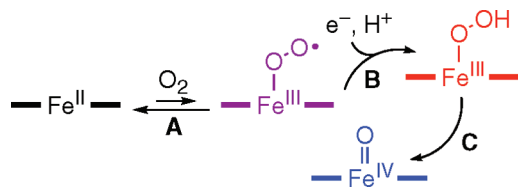


**Figure 2.** (a) UV/vis spectral changes showing the formation of **3** (red line) in the reaction of  $[\text{Fe}^{\text{II}}(\text{TMC})](\text{CF}_3\text{SO}_3)_2$  (0.5 mM) and  $\text{O}_2$  in the presence of BNAH (0.5 mM) and  $\text{HClO}_4$  (0.5 mM) in  $\text{CH}_3\text{CN}$  at 25 °C. (b) ESI MS spectrum of **3**. Peaks at  $m/z$  of 184.5 and 477.0 correspond to  $[\text{Fe}^{\text{IV}}(\text{TMC})(\text{O})(\text{CH}_3\text{CN})]^{2+}$  and  $[\text{Fe}^{\text{IV}}(\text{TMC})(\text{O})(\text{CF}_3\text{SO}_3)]^+$ , respectively. Insets show the observed (left panel) and calculated (right panel) isotope distribution patterns.

### Scheme 2



$[\text{Fe}^{\text{II}}(\text{N4Py})]^{2+}$  and  $[\text{Fe}^{\text{II}}(\text{Bn-TPEN})]^{2+}$ . This observation is in line with previous reports that only in alcohol or acetone are iron(III)-hydroperoxo complexes generated in the reactions of iron(II) complexes with  $\text{H}_2\text{O}_2$ .<sup>8,9</sup> Also, the spin states of the iron(II) complexes were shown to be different depending on solvents; a low-spin iron(II) complex formed in  $\text{CH}_3\text{CN}$ , whereas, in acetone, a high-spin iron(II) complex formed.<sup>8b</sup> We have also confirmed in the present study that  $[\text{Fe}^{\text{II}}(\text{N4Py})]^{2+}$  and  $[\text{Fe}^{\text{II}}(\text{Bn-TPEN})]^{2+}$  are low-spin complexes in  $\text{CH}_3\text{CN}$  while they are high-spin in  $\text{CH}_3\text{OH}$  (SI, Figure S6 for  $^1\text{H}$  NMR spectra). Further, cyclic voltammetric measurements indicate that the  $\text{Fe}^{\text{III/II}}$  redox potentials of high-spin iron(II) complexes are significantly lower than those of the corresponding low-spin iron(II) complexes. For example, the high-spin iron(II) complexes in  $\text{CH}_3\text{OH}$  show irreversible redox behavior at lower potentials ( $E_{\text{pc}} = 0.29$  V and  $E_{\text{pa}} = 0.63$  V vs SCE for  $[\text{Fe}^{\text{II}}(\text{N4Py})]^{2+}$  and  $E_{\text{pc}} = 0.29$  V and  $E_{\text{pa}} = 0.75$  V for  $[\text{Fe}^{\text{II}}(\text{Bn-TPEN})]^{2+}$ ), whereas the low-spin iron(II) complexes in  $\text{CH}_3\text{CN}$  show reversible behavior at higher potentials ( $E^{\text{O}} = 1.00$  V for  $[\text{Fe}^{\text{II}}(\text{N4Py})]^{2+}$  and  $E^{\text{O}} = 0.95$  V for  $[\text{Fe}^{\text{II}}(\text{Bn-TPEN})]^{2+}$ ) (SI, Figure S7 for cyclic voltammograms). In the case of  $[\text{Fe}^{\text{II}}(\text{TMC})]^{2+}$ , it is in a high-spin Fe(II) state in  $\text{CH}_3\text{CN}$  (0.38 V vs SCE).<sup>5</sup> Thus, the present results demonstrate that high-spin iron(II) complexes with a low  $\text{Fe}^{\text{III/II}}$  redox potential are able to bind and activate  $\text{O}_2$  to form iron–oxygen adducts in the presence of an NADH analogue and an acid. It is worth noting that it is high-spin Fe(II) species which bind and activate  $\text{O}_2$  in heme and nonheme iron enzymes and in bleomycin.<sup>2,13</sup>

A proposed mechanism for  $\text{O}_2$ -activation in the complexes described here is depicted in Scheme 2. The reaction is initiated by  $\text{O}_2$ -binding by a high-spin iron(II) complex that leads to the generation of an iron(III)-superoxo intermediate (pathway A); consecutive electron- and proton-transfer steps result in conversion to a low-spin iron(III)-hydroperoxo intermediate (pathway B). While iron(III)-hydroperoxo intermediates were formed as the final product in the reaction of iron complexes bearing pentadentate N4Py and Bn-TPEN ligands, the iron complex bearing a tetradentate TMC ligand afforded the iron(IV)-oxo complex via O–O bond cleavage in an unidentified  $[(\text{TMC})\text{Fe}^{\text{III}}-\text{OOH}]^{2+}$  intermediate (pathway C).<sup>14</sup>

In conclusion, we have reported the first example showing the generation of nonheme iron(III)-hydroperoxo and iron(IV)-oxo complexes by activating  $\text{O}_2$  with a biologically important electron donor, an NADH analogue, and an acid. The formation of the iron(III)-hydroperoxo and iron(IV)-oxo complexes was found to depend on the supporting ligands. We have also demonstrated that it is high-spin nonheme iron(II) complexes with low  $\text{Fe}^{\text{III/II}}$  redox potentials which are able to bind and activate  $\text{O}_2$  to generate iron–oxygen intermediates.

**Acknowledgment.** The research was supported by KOSEF/MEST through the CRI Program (to W.N.) and WCU Program (R31-2008-000-10010-0) (to S.F. and W.N.), KOSEF (R01-2008-000-20704-0) (to W.S.), and a Global COE program from the Ministry of Education, Culture, Sports, Science and Technology, Japan (to S.F.).

**Supporting Information Available:** Experimental details and spectroscopic and cyclic voltammetric data. This material is available free of charge via the Internet at <http://pubs.acs.org>.

### References

- (1) (a) Comba, P.; Kerscher, M.; Schiek, W. *Prog. Inorg. Chem.* **2007**, *55*, 613–704. (b) Kovacs, J. A.; Brines, L. M. *Acc. Chem. Res.* **2007**, *40*, 501–509. (c) Nam, W. *Acc. Chem. Res.* **2007**, *40*, 522–531. (d) Costas, M.; Mehn, M. P.; Jensen, M. P.; Que, L., Jr. *J. Chem. Rev.* **2004**, *104*, 939–986.
- (2) (a) Solomon, E. I.; Wong, S. D.; Liu, L. V.; Decker, A.; Chow, M. S. *Curr. Opin. Chem. Biol.* **2009**, *13*, 99–113. (b) Kovaleva, E. G.; Lipscomb, J. D. *Nat. Chem. Biol.* **2008**, *4*, 186–193. (c) Krebs, C.; Fujimori, D. G.; Walsh, C. T.; Bollinger, J. M., Jr. *Acc. Chem. Res.* **2007**, *40*, 484–492. (d) Abu-Omar, M. M.; Loaiza, A.; Hontzeas, N. *Chem. Rev.* **2005**, *105*, 2227–2252. (e) Ortiz de Montellano, P. R. *Cytochrome P450: Structure, Mechanism, and Biochemistry*, 3rd ed.; Kluwer Academic/Plenum Publishers: New York, 2005. (f) Denisov, I. G.; Makris, T. M.; Sliagar, S. G.; Schlichting, I. *Chem. Rev.* **2005**, *105*, 2253–2276.
- (3) (a) Shook, R. L.; Borovik, A. S. *Chem. Commun.* **2008**, 6095–6107. (b) Korendovych, I. V.; Kryatov, S. V.; Rybak-Akimova, E. V. *Acc. Chem. Res.* **2007**, *40*, 510–521. (c) Borovik, A. S. *Acc. Chem. Res.* **2005**, *38*, 54–61.
- (4) (a) Thallaj, N. K.; Rotthaus, O.; Benhamou, L.; Humbert, N.; Elhabiri, M.; Lachkar, M.; Welter, R.; Albrecht-Gary, A.-M.; Mandon, D. *Chem.–Eur. J.* **2008**, *14*, 6742–6753. (b) Korendovych, I. V.; Kryatov, O. P.; Reiff, W. M.; Rybak-Akimova, E. V. *Inorg. Chem.* **2007**, *46*, 4197–4211. (c) MacBeth, C. E.; Golombek, A. P.; Young, V. G., Jr.; Yang, C.; Kuczera, K.; Hendrich, M. P.; Borovik, A. S. *Science* **2000**, *289*, 938–941. (d) Kimura, E.; Kodama, M.; Machida, R.; Ishizu, K. *Inorg. Chem.* **1982**, *21*, 595–602.
- (5) Kim, S. O.; Sastri, C. V.; Seo, M. S.; Kim, J.; Nam, W. *J. Am. Chem. Soc.* **2005**, *127*, 4178–4179.
- (6) Thibon, A.; England, J.; Martinho, M.; Young, V. G., Jr.; Frisch, J. R.; Guillot, R.; Girerd, J.-J.; Muncie, E.; Que, L., Jr.; Banse, F. *Angew. Chem., Int. Ed.* **2008**, *47*, 7064–7067.
- (7) Abbreviations: TMC = 1,4,8,11-tetramethyl-1,4,8,11-tetraaza-cyclotetradecane, TMC-Py = 1-(2-pyridylmethyl)-4,8,11-trimethyl-1,4,8,11-tetraaza-cyclotetradecane, N4Py = *N,N*-bis(2-pyridylmethyl)-bis(2-pyridyl)methylamine, Bn-TPEN = *N*-benzyl-*N,N',N'*-tris(2-pyridylmethyl)-1,2-diaminoethane.
- (8) (a) Lubben, M.; Meetsma, A.; Wilkinson, E. C.; Feringa, B.; Que, L., Jr. *Angew. Chem., Int. Ed.* **1995**, *34*, 1512–1514. (b) Roelfes, G.; Lubben, M.; Chen, K.; Ho, R. Y. N.; Meetsma, A.; Genseberger, S.; Hermant, R. M.; Hage, R.; Mandal, S. K.; Young, V. G., Jr.; Zang, Y.; Kooijman, H.; Spek, A. L.; Que, L., Jr.; Feringa, B. L. *Inorg. Chem.* **1999**, *38*, 1929–1936.
- (9) (a) Hazell, A.; McKenzie, C. J.; Nielsen, L. P.; Schindler, S.; Weitzer, M. *J. Chem. Soc., Dalton Trans.* **2002**, 310–317. (b) Simaan, A. J.; Döpner, S.; Banse, F.; Bourcier, S.; Bouchoux, G.; Boussac, A.; Hildebrandt, P.; Girerd, J.-J. *Eur. J. Inorg. Chem.* **2000**, 1627–1633.
- (10) Fukuzumi, S.; Koumitsu, S.; Hironaka, K.; Tanaka, T. *J. Am. Chem. Soc.* **1987**, *109*, 305–316.
- (11) We have previously shown that the iron–oxygen intermediates such as iron(III)-hydroperoxo and iron(IV)-oxo species react further with BNAH (i.e., in hydride-transfer reactions); see: Fukuzumi, S.; Kotani, H.; Lee, Y.-M.; Nam, W. *J. Am. Chem. Soc.* **2008**, *130*, 15134–15142. Also, see SI, Figure S3b.
- (12) Rohde, J.-U.; In, J.-H.; Lim, M. H.; Brennessel, W. W.; Bukowski, M. R.; Stubna, A.; Münck, E.; Nam, W.; Que, L., Jr. *Science* **2003**, *299*, 1037–1039.
- (13) (a) Decker, A.; Solomon, E. I. *Curr. Opin. Chem. Biol.* **2005**, *9*, 152–163. (b) Burger, R. M. *Struct. Bonding (Berlin)* **2000**, *97*, 287–303.
- (14) We have previously proposed that the formation of  $[(\text{TMC})\text{Fe}^{\text{IV}}(\text{O})]^{2+}$  (**3**) from the reaction of  $[\text{Fe}^{\text{II}}(\text{TMC})]^{2+}$  and  $\text{O}_2$  in solvent mixtures of  $\text{CH}_3\text{CN}$ /alcohols or  $\text{CH}_3\text{CN}$ /ethers occurs via O–O bond cleavage of a ( $\mu$ -1,2-peroxo)diiron(III) intermediate; see ref 5.

JA905691F